Talanta 122 (2014) 278–284

Contents lists available at ScienceDirect

Talanta

journal homepage: www.elsevier.com/locate/talanta

Dendrimer-grafted graphene oxide nanosheets as novel support for trypsin immobilization to achieve fast on-plate digestion of proteins ☆

Bo Jiang [a,b,c], Kaiguang Yang [b], Lihua Zhang [b,*], Zhen Liang [b], Xiaojun Peng [a], Yukui Zhang [b]

[a] State Key Laboratory of Fine Chemicals, Dalian University of Technology, Dalian 116012, China
[b] National Chromatographic R&A Center, Key Laboratory of Separation Science for Analytical Chemistry, Dalian Institute of Chemical Physics, Chinese Academy of Science, Dalian 116023, China
[c] University of Chinese Academy of Sciences, Beijing 100039, China

ARTICLE INFO

Article history:
Received 24 October 2013
Received in revised form
22 January 2014
Accepted 25 January 2014
Available online 1 February 2014

Keywords:
Graphene oxide
Dendrimer
On-plate digestion
Proteomics
IMER

ABSTRACT

In this study, dendrimer grafted graphene oxide nanosheets (dGO) were prepared by covalent reaction. The successful synthesis of dGO was confirmed by Fourier-transform infrared spectra, Raman spectra, Thermo gravimetric analysis and *Zeta* potential. Taking advantages of large surface area, excellent biocompatibility and abundant functional groups, dGO provided an ideal substrate for trypsin immobilization. Trypsin-linked dGO was synthesized through covalent bonding using glutaraldehyde as coupling agents. The amount of trypsin immobilized on dGO nanosheets was calculated to be about 649 ± 20 mg/g. The activity of immobilized trypsin could be maintained for over 10 days at 4 °C. On-plate proteolysis could be performed without removing trypsin-linked dGO, because dGO did not interfere with matrix-assisted laser desorption ionization time-of-flight tandem mass spectrometry analysis. By such an immobilized enzymatic reactor, standard proteins could be efficiently digested within 15 min, with sequence coverages comparable or better than those obtained by conventional over-night in-solution digestion. Furthermore, trypsin-linked dGO showed high sensitivity when applied to trace samples analysis. All these results demonstrated that the developed dGO based enzymatic reactor might provide a promising tool for high throughput proteome identification.

1. Introduction

One of the most important tasks of proteomics is to develop efficient and rapid approaches to identify various proteins [1,2]. Enzymatic cleavage coupled with matrix-assisted laser desorption ionization time-of-flight tandem mass spectrometry (MALDI-TOF MS) is a powerful technique for effective protein identification [3,4]. For MALDI-TOF MS detection, the rapid and complete digestion of proteins is crucial to achieve the high throughput and accurate protein identification [5]. However, sample pretreatment prior to MALDI-TOF MS analysis is often time-consuming, resulting in low analytical throughput. Furthermore, sample loss during the multi-step transfer is inevitable, which could lead to the low identification efficiency for proteins [6]. Therefore, the successful MALDI-TOF MS analysis requires the acceleration of enzymatic digestion and the simplification of sample preparation procedures. Immobilized enzyme reactors (IMER), as an alternative to traditional in-solution digestion, possess the advantage of tolerance for high enzyme to protein ratio, resulting in short digestion time and low risk for enzyme autolysis [7,8]. Furthermore, on-plate proteolysis could simplify sample preparation procedure and reduce sample loss [9]. Therefore, IMER coupled with on-plate proteolysis has been considered as a potential solution to solve the above-mentioned problems [10,11].

For on-plate digestion, the support used for enzyme immobilization plays a key role. To date, several matrixes have been successfully used for on-plate digestion. Li et al. developed a novel on-plate digestion method using magnetic nanospheres as support for trypsin immobilization. Compared to traditional in solution digestion, the digestion time was significantly reduced to 5 min [9]. However, the magnetic nanoparticles must be removed from MALDI plate before MS analysis, to eliminate the interference on MS signals of peptides, which inevitably increased the risk of sample loss. Although with carbon nanotube as the support, the immobilized enzyme amount could be increased, the poor dispersibility would interfere the crystal formation of matrix and peptides, which might significantly decrease MS signals [10]. Therefore, it is urgently required to develop novel supports which could simultaneously provide high enzyme immobilization

* Corresponding author. Fax: +86 411 84379720.
E-mail address: lihuazhang@dicp.ac.cn (L. Zhang).

0039-9140/$ - see front matter © 2014 Elsevier B.V. All rights reserved.
http://dx.doi.org/10.1016/j.talanta.2014.01.056

amount, excellent dispersibility and non-interference with MALDI analysis.

Graphene oxide (GO), one of the most important derivatives of graphene, has recently attracted increasing attention in biological fields, such as biological imaging [12,13], drug/gene delivery [14–16], and biosensing [17–19], due to its large surface area and good biocompatibility. Furthermore, GO possesses abundant functional groups on its surface, such as carboxylic acids, hydroxyl, carbonyl and epoxy groups, facilitating chemical modifications [20–22]. GO has been successfully used as MALDI-TOF MS matrix for the analysis of small molecules [23], indicating no interference with MALDI analysis. The above-mentioned advantages make GO of great superiority as the candidate for enzyme immobilization to achieve on-plate digestion.

Up till now, several GO-based IMER were successfully prepared for rapid and efficient proteolysis. Chen et al. developed an efficient microchip proteolysis by immobilizing trypsin in the layer-by-layer coating of GO and chitosan on in-channel glass fiber [24]. We also prepared magnetic GO based IMER, in which trypsin was immobilized via π–π stacking and hydrogen bonding interaction [25]. Although high efficient digestion was obtained in both cases, trypsin desorption occurred inevitably because trypsin was attached on GO via non-covalent bonding. Recently, trypsin was further covalently bonded on polymers functionalized GO [26] and microchip channel with GO coating [27]. However, the active sites of trypsin might be well exposed with fragile cross-linkers introduced between GO and enzymes.

Recently, dendrimer has received more and more attention in biological fields due to its defined hyperbranched nanoarchitecture, excellent biocompatibility and large amount of functional groups at the periphery [28–31]. Furthermore, well-organized and close-packed arrays of dendrimer could be formed on GO surface, leading to the improved dispersibility of GO in water [32]. Due to the hyperbranched nanoarchitecture of dendrimer, enzyme could not be wrapped by the fragile chains, beneficial to avoid the mask of its active sites and decrease the risk of enzyme autolysis [33]. Besides, with abundant functional groups at the periphery of dendrimer, the immobilized amount of enzyme could be obviously improved [34]. Therefore, it could be envisaged that dendrimer-grafted GO (dGO) provides superiority of good dispersibility, hyperbranched nanoarchitecture and high capacity for enzyme immobilization. Herein, to the best of our knowledge, for the first time, dGO was prepared by covalent bonding and used as probe for trypsin immobilization with glutaraldehyde as coupling agents. The prepared trypsin-linked dGO was successfully applied to on-plate protein digestion, and showed great potential in large-scale proteome analysis.

2. Experimental

2.1. Chemicals and materials

GO was obtained from Xianfeng Nanotech Port (Nanjing, China). 1-Ethyl-3-(3-dimethylaminopropyl) carbodiimide (EDC), *N*-hydroxysulfosuccinimide (NHS), 2-morpholino-ethanesulfonic acid (MES), TPCK-treated trypsin, dithiothreitol (DTT), iodoacetamide (IAA), formic acid (FA), bovine serum albumin (BSA), myoglobin (Myo), cytochrome *c* (Cyt-*c*), sodium cyanoborohydride ($NaCNBH_3$), glutaraldehyde (GA, 50 wt%), manganese chloride ($MnCl_2$), dendrimer (G2.0) and trifluoroacetic acid (TFA) were purchased from Sigma Chemical (St. Louis, MO, USA). Acetonitrile (ACN) was purchased from Merck (Darmstadt, Germany). Enhanced BCA protein assay kit was provided by Beyotime Biotech (Nantong, China). A-Cyano-4-hydroxy-cinnamic acid (CHCA) was obtained from Bruker (Daltonios, Germany).Water was purified using a Milli-Q system (Millipore, Molsheim, France). Other chemicals and analytically pure reagents were used as received.

2.2. Preparation of dGO

Under optimal conditions, 10 mg GO in 10 mL of 2-morpholino-ethanesulfonic acid solution (MES, 0.1 M, pH 5.6) was ultrasonicated for 3 h to obtain uniform dispersion. Then, 5 mg of EDC and 4 mg of NHS were added, and stirred for another 30 min at room temperature to activate carboxyl groups of GO. Next, 200 μL methanol solution of dendrimer with an ethylenediamine core was continuously dropped within 30 min. Afterwards, the mixture was stirred vigorously for another 2 h at room temperature to accelerate the reaction. Finally, dGO nanosheets were purified with a dialyzer (10 K molecular weight cutoff) using coupling buffer (50 mM NH_4OAc, 1 mM $CaCl_2$, 1 mM $MnCl_2$, pH ~ 8.3) to remove the excessive dendrimer.

2.3. Preparation of trypsin-linked dGO

One milligram dGO was transferred to a 1.5 mL Eppendorf tube, and the amino group of dGO was activated at room temperature under gentle rotation for 1.5 h by adding 1 mL 10 wt% GA solutions in coupling buffer. GA modified dGO was then collected by centrifugation at 20,000 rpm. Followed by four times washing with coupling buffer, GA modified dGO was incubated with 1 mg TPCK-treated trypsin, dissolved in 1 mL coupling buffer containing 1 wt% $NaCNBH_3$, for 3 h under rotation. After the removal of the excessive trypsin solution, the product was incubated for 1 h with 1 mL 0.75 wt% glycine/1 wt% $NaCNBH_3$ in coupling buffer. Finally, the obtained trypsin-linked dGO was washed four times with coupling buffer, followed by dissolving in 50 mM NH_4HCO_3 (pH 8.0), and storing at 4 °C as the stocking solution.

2.4. Standard protein preparation

Standard proteins (BSA, Cyt-*c*, Myo) dissolved in 1 mL 50 mM NH_4HCO_3 (pH 8.0) were denatured at 90 °C for 20 min, and then reduced in 10 mM DTT for 2 h at 56 °C. After cooled to room temperature, cysteines were alkylated in the dark in 20 mM IAA for 1 h at 37 °C. The obtained protein solution was used for on-plate and in-solution digestion, respectively.

2.5. On-plate and in-solution digestion

Each diluted protein solution (0.5 μL) was deposited on the plate of a MALDI-TOF MS (Bruker Ultraflex III). After that, 0.5 μL of trypsin-linked dGO stock solution was spotted, aspirated and dispensed for 5–10 cycles with pipette tip. The MALDI plate was then placed in a home-built humidity chamber, and incubated at 37 °C for 15 min. Subsequently 0.5 μL CHCA (7 mg/mL) was added to the digests. For comparison, in-solution digestion was performed in NH_4HCO_3 buffer (50 mM, pH 8.0) with enzyme to protein ratio (*m*/*m*) at 1:40 at 37 °C for 12 h, before 2 μL FA was added to terminate the digestion.

2.6. Human plasma preparation and digestion

The human plasma sample was thawed at −20 °C and ultrafiltrated at 134,000*g* for 60 min. A multiple affinity removal column (4.6 × 50 mm, Hu-14) was used to remove 14 high-abundant proteins. The obtained low-abundant proteins were desalted by a C8 trap column, and dissolved in 50 mM NH_4HCO_3 (pH 8.0) containing 8 M urea. The concentration of the low-abundant proteins was determined as 1 mg/mL by BCA reagents.

Proteins were dissolved in 50 mM NH_4HCO_3 (pH 8.0) containing 8 M urea, and then reduced in 10 mM DTT for 1 h at 56 °C. When cooled to room temperature, cysteines were alkylated in the dark in 20 mM IAA for 30 min at 37 °C, followed by dilution with 50 mM NH_4HCO_3 (pH 8.0) to decrease the urea concentration below 1 M. The sample was desalted on an SPE-C8 column with 2 and 98% ACN (*v*/*v*) as the loading and eluting buffer, respectively. The eluants were lyophilized in a SpeedVac (Thermo Fisher, San Jose, CA, USA), and redissolved in 50 mM NH_4HCO_3 (pH 8.0) to desired concentration. Trypsin-linked dGO was transferred to 20 μg of protein solution (20 μL, *E*/*S* 5:1) in a 1.5 mL Eppendorf tube. After 60 min digestion at 37 °C, 2 μL of FA was added into the solution to terminate the reaction. The supernatant was analyzed by *nano*RPLC-ESI-MS/MS. In-solution digestion was performed by adding trypsin into the pretreated protein sample with a substrate-to-enzyme ratio of 40:1 (*m*/*m*), and the solution was incubated at 37 °C for 12 h.

2.7. MS analysis

All MALDI mass spectra were taken from an Ultraflex III MALDI-TOF/TOF instrument equipped with a high rep rate (100 Hz) diodepumped all-solid-state SmartBeam laser (third harmonic at 355 nm). The analysis was performed under positive reflection mode, with signal averaging of 1000 laser shots. The laser intensity was kept constant for all samples after optimization. Calibration of MALDI-TOF/TOF MS spectra was performed with ten commercial peptides. Peptide mass fingerprint (PMF) was searched via version 3.2 with database (462,764 sequence; 163,773,385 residues). Other search parameters were set as follows: enzyme, trypsin; fixed modifications, carbamidomethyl (C); allow up to 2 missed cleavage; peptide mass tolerance, 100 ppm.

The digests of human plasma proteome were injected for *nano*-LC-ESI–MS/MS analysis. A packed C_{18} column (75 μm i.d. × 15 cm) was used for peptide separation, with the flow rate of 200 nL/min. Two percent (*v*/*v*) ACN with 0.1% (*v*/*v*) FA (buffer A) and 98% (*v*/*v*) ACN with 0.1% (*v*/*v*) FA (buffer B) were used to generate a 125 min gradient, set as follows: 0% B for 10 min, to 5% B in 15 min, to 35% B in 105 min, to 80% B in 115 min, and kept at 80% B for 10 min. The LTQ-Orbitrap instrument (Thermo-Fisher, San Jose, CA, USA) was operated at positive ion mode. The spray voltage was 2.3 kV, and the heated capillary temperature was 200 °C. Total ion current chromatograms and mass spectra covering the mass range from *m*/*z* 350 to 1800 were recorded with Xcalibur software (version 1.4). MS/MS spectra were acquired by data-dependent acquisition mode with 15 precursor ions selected from one MS scan. Precursor selection was based on parent ions intensity, and the normalized collision energy for MS/MS scanning was 35%.

For nanoRPLC-ESI–MS/MS analysis, protein identification was performed with a local installation MASCOT of version 2.4. The database was ipi.Huaman.v3.7.8, and reversed sequences were appended to the database for the evaluation of false discovery rate (FDR). Cysteine residues were searched as static modification of 57.0215 Da. Peptides were searched using fully tryptic cleavage constraints, and up to two internal cleavages sites were allowed for tryptic digestion. The mass tolerances were 10 ppm for parent masses and 0.5 Da for fragment masses. The search results were filtered by pBuild to control the peptide FDR $\leq$ 1%.

2.8. Characterization

Fourier-transform infrared (FT-IR) spectra were recorded on Perkin-Elmer Spectrum GX spectrometer (Perkin-Elmer, Waltham, USA). Thermo Gravimetric Analysis (TGA) was conducted with Netzsch STA449F3 thermal analyzer (Netzsch, Bavaria, Germany) that was fitted to a nitrogen purge gas at 10 °C/min heating rate. Raman spectroscopy was also used to characterized GO (532 nm excitation line, Home-made, Dalian Institute of Chemical Physics, Dalian, China). Transmission electron microscopy (TEM) images were obtained by JEOL JEM-2000 EX transmission electron microscope at

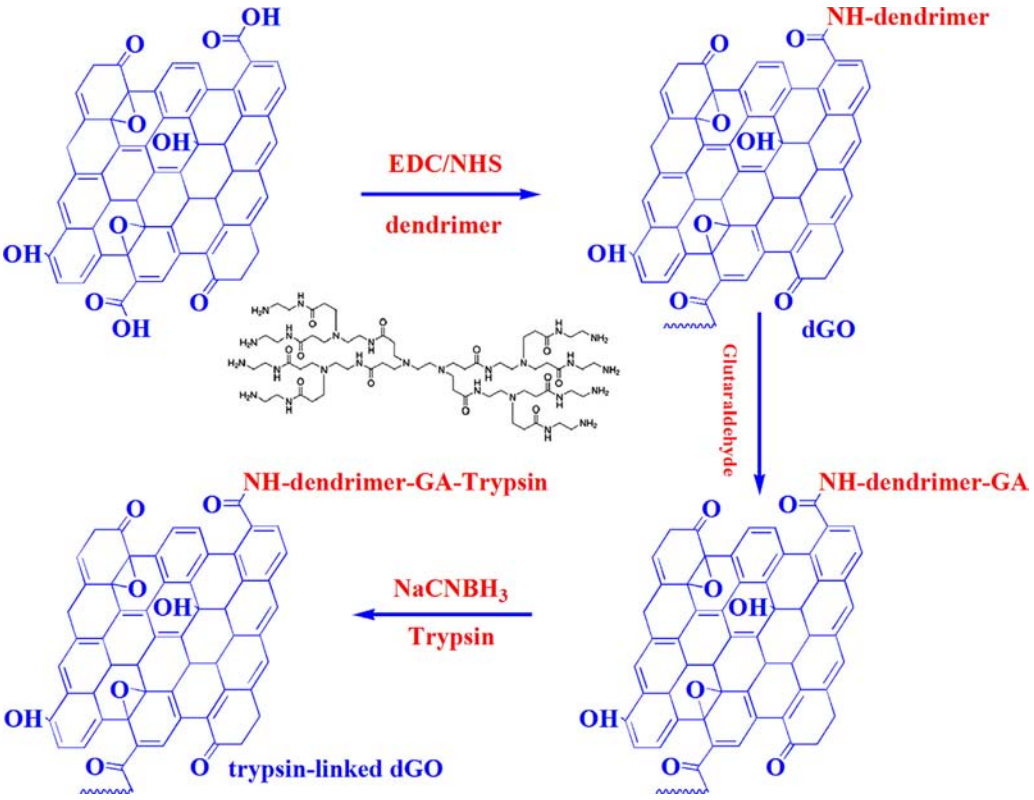

Scheme 1. Schematic illustration of trypsin immobilization onto dGO.

120 KV (JEOL, Tokyo, Japan). *Zeta* potential was detected by Marvern Nano-ZS90 Zeta Sister (Marvern, Worcestershire, UK). The concentration of enzyme was detected by Enhanced BCA protein assay kit with Multiskan MK3 Thermo Labsystems (Thermo, Waltham, MA, USA).

3. Results and discussion

3.1. Synthesis of dGO and trypsin-linked dGO nanosheets

GO possesses abundant oxide-containing groups on its surface, facilitating further functional modification [35]. In this work, covalent bonding method was used to prepare dGO and trypsin-linked dGO nanosheets. The schematic illustration of dGO and trypsin-linked dGO nanosheets was shown in Scheme 1. First, amino-terminated dendrimer was covalently assembled to the surface of GO through forming new amide bond with the aid of EDC and NHS. The prepared dGO nanosheets were applied as a novel support for immobilizing enzyme. Then, glutaraldehyde, as cross-linker, was bonded to the surface of dGO through reacting with the rudimental amino group of dGO. Finally, trypsin was immobilized on glutaraldehyde modified dGO *via* the reaction between the amino group of trypsin and the aldehyde group of glutaraldehyde. The prepared trypsin-linked dGO was used as IMER for on-plate digestion.

3.2. Characterization of dGO

FT-IR spectra were used to characterize the prepared dGO nanosheets. As shown in Fig. 1, for GO, the peak around 1728 cm^{-1} corresponds to C=O stretching vibration of the carboxylic group, and that at 1622 cm^{-1} is due to C=C stretch mode [36]. The dendrimer exhibits two strong absorption bands centered at 1647 and 1551 cm^{-1}, assigned to the C=O stretching (amide I) and N–H bending (amide II) vibrations, respectively. When converted to dGO, the peak at 1728 cm^{-1}almost disappears, and the new peaks appear at 2928 and 2855 cm^{-1}, corresponding to C–H stretch of dendrimer [32]. In addition, new amide adsorption peaks at 1646 and 1542 cm^{-1} are also found. These results verify that dendrimer is covalently assembled to GO surface.

Fig. 2 shows the typical Raman spectra of GO and dGO nanosheets, in which the peak around 1355 cm^{-1} (D-band) is in correspondence with vibrations of carbon atoms with dangling bonds in plane terminations of disordered graphite. The peak around 1590 cm^{-1} (G-band) could be attributed to the vibration of sp^2-bonded carbon atoms in a two-dimensional hexagonal lattice

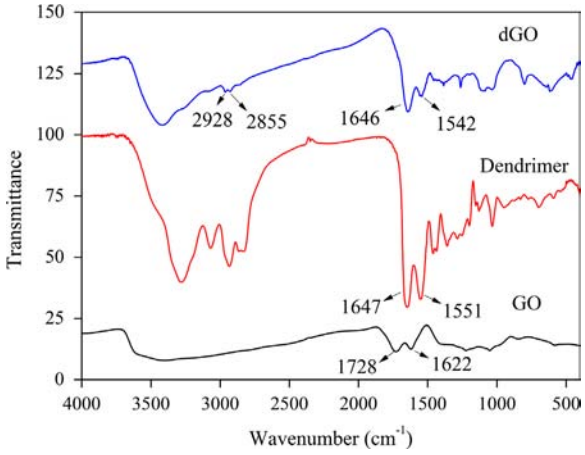

Fig. 1. FT-IR spectra of GO, dendrimer and dGO.

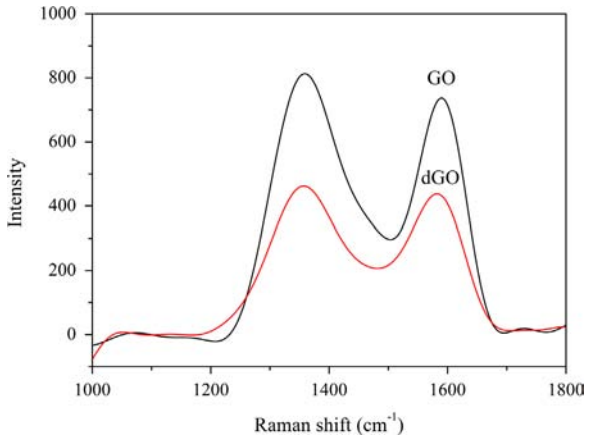

Fig. 2. Raman spectra of GO and dGO.

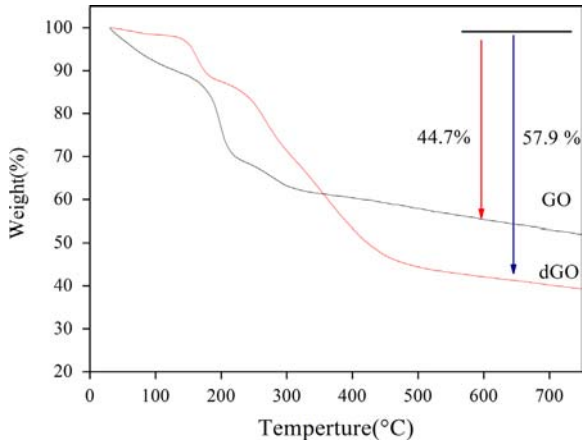

Fig. 3. TGA curves of GO and dGO.

[37]. When converted to dGO, the intensity ratio of D over G band (I_D/I_G, 1.06) is lower than that of GO (1.10), indicating that more sp^2 domains are formed during the covalent reaction, in accordance with previous research [38]. The Raman spectra also reinforce the successful synthesis of dGO nanosheets.

Thermo gravimetric analysis (TGA) was applied to determine the quantitative composition of dGO nanosheets. As shown in Fig. 3, for GO, its main mass loss takes place around 200–450 °C, corresponding to the pyrolysis of labile oxygen-containing groups. There is also a mass loss (7%) below 100 °C, which could be resolved as the removal of stored water in its π–π stacked structure [39]. As for the curve of dGO, compared with that of GO, its decomposition shows the similar trend as GO. With the consideration on the data at 600 °C, the content of dendrimer is about 13.2 wt%. Such high immobilization amount should be attributed to the ultra-high surface area of GO and abundant functional groups on GO surface [40], since the large number of amino groups at the periphery of dendrimer not only enhance the dispersibility, but also impart excellent biocompatibility for dGO. Furthermore, dendrimer may not wrap around enzymes to mask their active sites because of their defined hyperbranched nanoarchitecture [32]. Therefore, dGO could be considered as a wonderful support for trypsin immobilization.

3.3. Evaluation of trypsin-linked dGO nanosheets

The surface charges of GO before and after grafted with dendrimer are -45.6 ± 8.04 mV and 40.8 ± 3.0 mV, respectively,

demonstrating the presence of abundant amino groups on dGO surface. The existing terminal amino groups ensure the covalent bonding of trypsin on dGO through coupling agent. The amount of immobilized trypsin on dGO surface reaches 649 ± 20 mg/g, much higher than that obtained with previously reported carbon nanotube [10]. The high immobilization amount should be attributed to the abundance of functional groups and hyperbranched nanoarchitecture of dGO. The morphology of the obtained trypsin-linked dGO was characterized by transmission electron microscopy (TEM). As shown in Fig. 4, trypsin-linked dGO nanosheets were well-dispersed in water, preferable for digestion.

In summary, as a novel IMER, trypsin-linked dGO nanosheets have several advantages. First, the good water-solubility of trypsin-linked dGO ensures the comprehensive contact between proteins and immobilized trypsin, accelerating proteolysis rate. Second, with hyperbranched nanoarchitecture of dGO, enzyme could not be wrapped by fragile chains of dendrimer, beneficial to avoid masking the active sites of enzyme. Finally, compared with non-covalent method, trypsin is fixed on dGO through covalent bonding, which could greatly reduce the risk of auto-digestion and trypsin desorption.

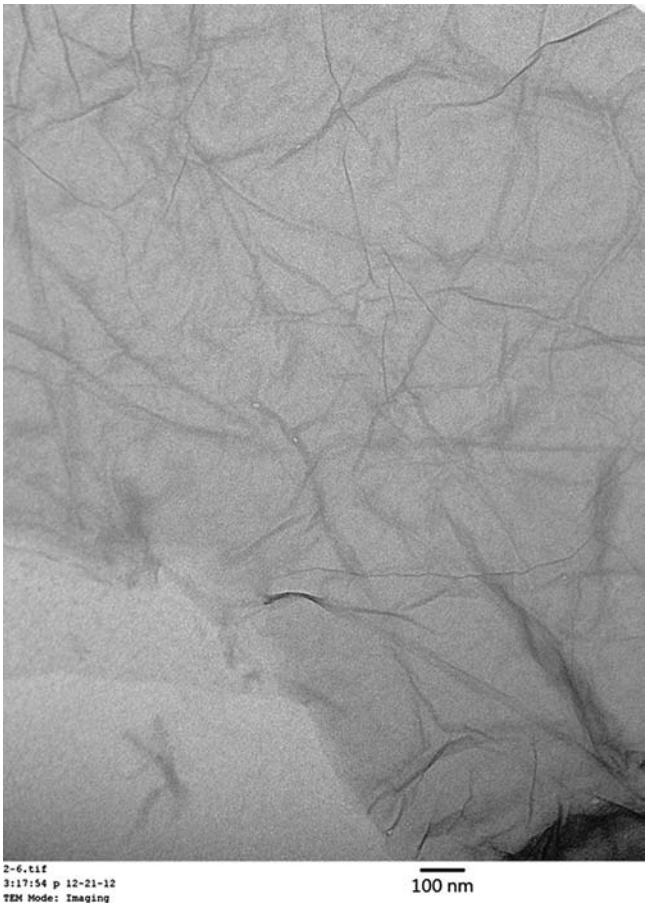

Fig. 4. TEM image of trypsin-linked dGO.

3.4. Effect of trypsin-linked dGO on MS signal

For on-plate digestion, IMER should not interfere with MS analysis. Herein, the tryptic digests of Myo with and without trypsin-linked dGO added was analyzed by MALDI-TOF MS, respectively. As shown in Fig. 5, in both cases, the analyte and the matrix formed homogeneously crystals. The identified peptide number and the signal intensity of Myo digests between two spectra showed no significant difference (Fig. 6), demonstrating that trypsin-linked dGO did not interfere with MALDI-TOF MS analysis. Thereby, MS analysis can be performed after on-plate proteolysis without the removal of trypsin-linked dGO, which could not only accelerate protein identification, but also avoid sample loss or contamination, especially advantageous for trace sample analysis.

3.5. On-plate protein digestion by trypsin-linked dGO

To enhance digestion efficiency and simplify the sample preparation, trypsin-linked dGO was used to perform on-plate digestion followed by MALDI-TOF MS analysis (Scheme 2). To ensure the complete digestion of proteins in a short time, the enzyme/substrate ratio (*E*/*S*) was optimized. With the incubation time set as 15 min at 37 °C, different amounts of trypsin-linked dGO were added to 0.5 μL of Cyt-*c* (100 ng/μL) solution. As shown in Fig. 7, with the *E*/*S* varied from 1:20 to 1:1, the intact Cyt-*c* was found, indicating insufficient digestion. However, when *E*/*S* was increased to 5:1, the intact Cyt-*c* peak disappeared. As shown in Fig. 8, in the digests of Cyt-*c*, the large peptide peaks with *m*/*z* over 2500 also disappeared. All these results indicated the complete digestion of Cyt-*c*, in accordance with the published criteria [41]. Furthermore, no peaks of auto-digested enzyme were found. Therefore, the *E*/*S* was set at 5:1 in the following experiments.

The feasibility and efficiency of on-plate proteolysis with trypsin-linked dGO were further demonstrated by the digestion of the mixture of BSA, Cyt-*c* and Myo. For comparison, the digestion of these three proteins was also performed by conventional in-solution digestion. The data shown in Table 1 demonstrated that the digestion efficiency of on-plate digestion was

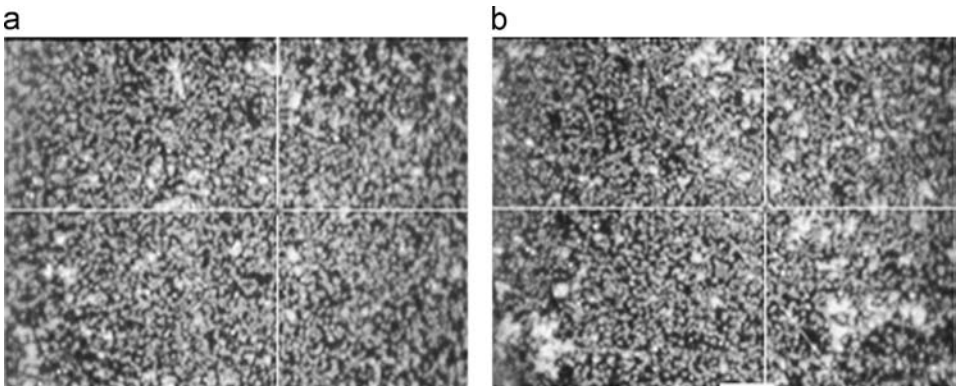

Fig. 5. Digital photographs of prepared Myo digests spots with (a) and without (b) trypsin-linked dGO added. On each spot, 0.5 μL Myo sample solution and 0.5 μL CHCA solution were spotted.

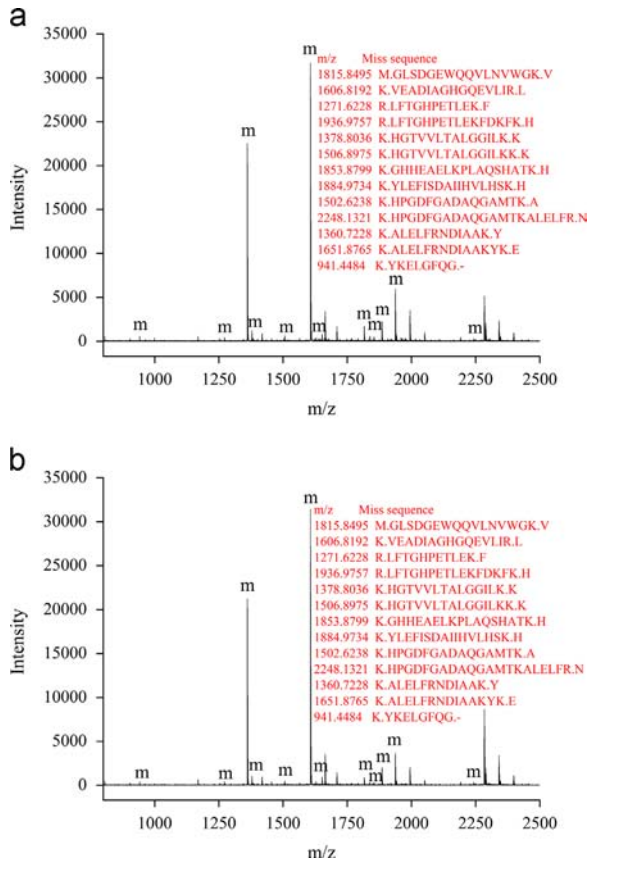

Fig. 6. MALDI-TOF mass spectra of the digests of Myo (A) with and (B) without dGO added in matrix. On each spot, 0.5 μL of Myo (50 ng/μL) and 0.5 μL of CHCA were mixed with pipette. m, Peptide from Myo.

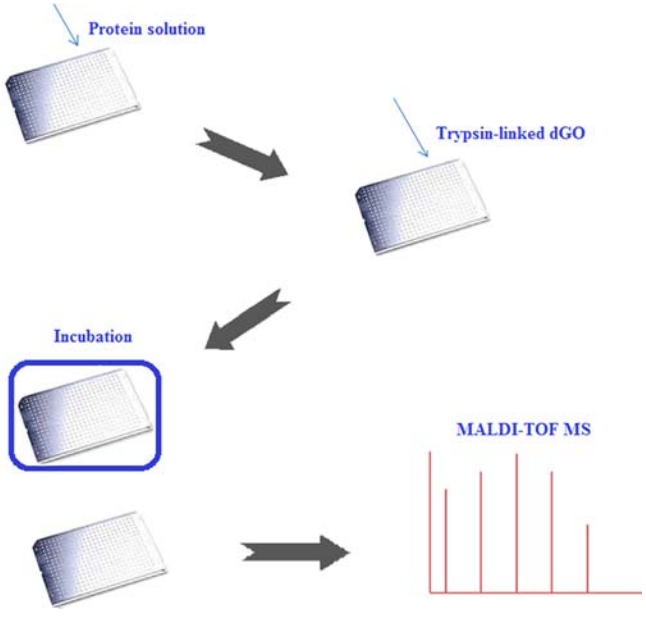

Scheme 2. Procedure of the on plate digestion by trypsin-linked dGO nanosheets.

comparable to that of the conventional in solution digestion, but the digestion time was significantly reduced from 12 h to only 15 min. The rapid digestion should be attributed to the increased *E*/*S* ratio by trypsin-linked dGO.

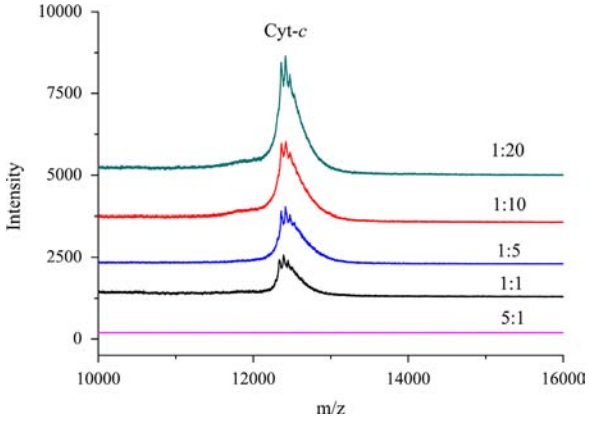

Fig. 7. MALDI-TOF mass spectra of the tryptic digest of Cyt-*c* (100 ng/μL, 0.5 μL) with different *E*/*S* ratios. The peaks marked correspond to the singly charged protein Cyt-*c*.

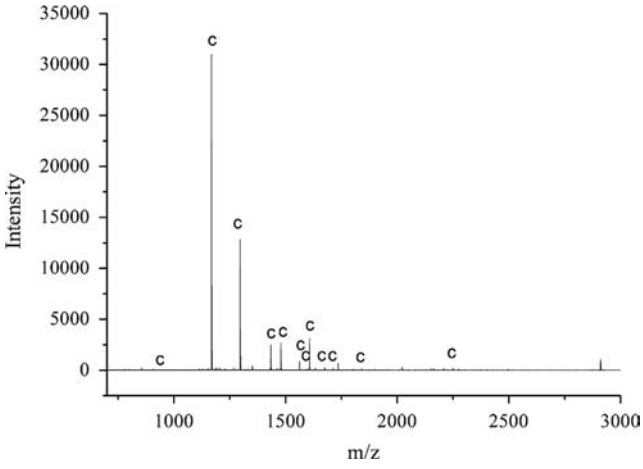

Fig. 8. MALDI-TOF mass spectra of the digests of Cyt-*c* obtained by on-plates digestion with *E*/*S* as 5:1. c, Peptide from Cyt-*c*.

Myo was further used to evaluate the effect of digestion time on the digestion efficiency of trypsin-linked dGO. Even if the digestion time was decreased to only 5 min, still 13 peptides were identified with amino acid sequence coverage as high as 84%, indicating the high throughput of on-plate digestion by dGO based IMER.

Since our developed trypsin-linked dGO did not inhibit MALDI-TOF MS signal, the removal of immobilized enzyme after on-plate digestion was unnecessary. Therefore, sample loss or contamination could be avoided, making the IMER especially suitable for trace sample analysis. Herein, with 150 fmol Myo chosen as the sample samples, as shown in Fig. 9, nine peptides were matched, with the corresponding amino-acid sequence coverage as 53%, demonstrating the ability of such an IMER for trace sample digestion.

To evaluate the stability of IMER, trypsin-linked dGO was stored at 4 °C for 10 d. The obtained sequence coverage of Myo still reached to 84%, equivalent to that obtained by freshly made IMER. Such good stability should be attributed to the excellent biocompatibility of dGO. The batch-to-batch reproducibility of protein digestion by trypsin-linked dGO was also evaluated, and the RSD for the sequence coverage of Myo was only 1.38% ($n=5$), indicating the good preparation reproducibility of trypsin-linked dGO.

To verify the digestion capacity of trypsin-linked dGO in large-scale proteome research, proteins extracted from human plasma were digested by trypsin-linked dGO, followed by *nano*RPLC-ESI–MS/MS

Table 1
MALDI-TOF MS results obtained by on-plate and in-solution digestion ($n=3$).

Protein	BSA (100 ng/μL)		Cyt-*c* (100 ng/μL)		Myo (100 ng/μL)	
Digestion method	On-plate	In-solution	On-plate	In-solution	On-plate	In-solution
Digestion time	15 min	12 h	15 min	12 h	15 min	12 h
Sequence Coverage (%)	55.3 ± 2.5	48.7 ± 1.5	67 ± 0	59 ± 2.6	84.3 ± 0.6	82.7 ± 2.9
Peptides matched	37 ± 2.6	26 ± 1	12 ± 0	12 ± 1.7	14 ± 0	14.3 ± 1.5

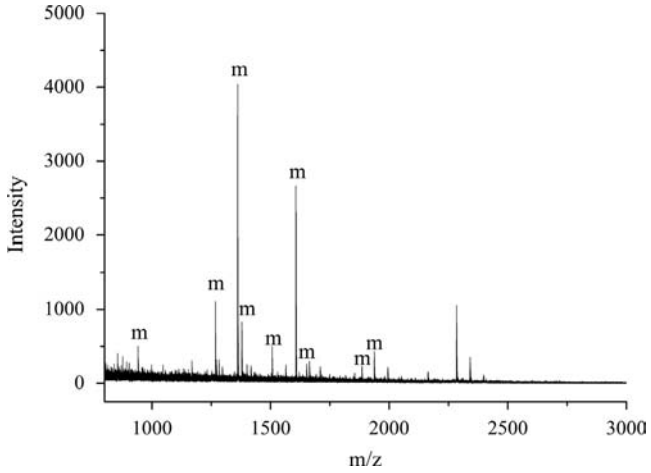

Fig. 9. MALDI-TOF mass spectrum of the digests of 150 fmol Myo obtained by on-plate digestion. All matched peptides are marked with "m".

analysis. Our experimental results showed that, by 1 h digestion, in total 125 protein groups were identified from 2 μg sample, more than those obtained by 12 h in-solution digestion (105 protein groups), among which 84 protein groups were identified by two methods. Such results suggest that our prepared dGO based IMER is of high digestion capacity even for complex biological samples, beneficial to increase the analysis throughput of proteomes.

4. Conclusions

In summary, trypsin-linked dGO was prepared and used as a novel IMER for on-plate digestion of proteins. Due to the good dispersibility, excellent biocompatibility, large enzyme loading capacity and no interference with MS signal, highly efficient and rapid protein digestion was obtained. Within only 15 min, protein could be efficiently digested with sequence coverage comparable to that obtained by conventional over-night in-solution digestion. The work not only offered a novel platform for high-speed on-plate proteolysis, but also opened a new field for applications of graphene.

Acknowledgements

This work was supported by National Basic Research Program of China (2012CB910601), National Nature Science Foundation (21190043 and 21005078), Creative Research Group Project by NSFC (21321064), and Innovation Method Fund of China (2012IM030400).

References

[1] A. Shevchenko, H. Tomas, J. Havliš, J.V. Olsen, M. Mann, Nat. Protoc. 1 (2006) 2856–2860.
[2] W. Qin, Z. Song, C. Fan, W. Zhang, Y. Cai, Y. Zhang, X. Qian, Anal. Chem. 84 (2012) 3138–3144.
[3] H. Geyer, S. Schmitt, M. Wuhrer, R. Geyer, Anal. Chem. 71 (1999) 476–482.
[4] A.J. Ibáñez, A. Muck, Y. Halim, A. Svatoš, J. Proteome Res. 6 (2007) 1183–1189.
[5] S. Wang, H. Bao, L. Zhang, P. Yang, G. Chen, Anal. Chem. 80 (2008) 5640–5647.
[6] J. Ma, L. Zhang, Z. Liang, Y. Shan, Y. Zhang, Tren, Anal. Chem. 30 (2011) 691–702.
[7] D.S. Peterson, T. Rohr, F. Svec, J.M.J. Fréchet, J. Proteome Res. 1 (2002) 563–568.
[8] G. Massolini, E. Calleri, J. Sep. Sci. 29 (2005) 7–21.
[9] Y. Li, B. Yan, C. Deng, J. Tang, J. Liu, X. Zhang, Proteomics 7 (2007) 3661–3671.
[10] Y. Zhang, W. Cao, M. Liu, S. Yang, H. Wu, H. Lu, P. Yang, Mol. BioSyst. 6 (2010) 1447–1449.
[11] S. Wang, H. Bao, L. Zhang, P. Yang, G. Chen, Anal. Chem. 80 (2008) 5640–5647.
[12] X. Sun, Z. Liu, K. Welsher, J.T. Robinson, A. Goodwin, S. Zaric, H. Dai, Nano Res. 1 (2008) 203–212.
[13] L. Deng, L. Liu, C. Zhu, D. Li, S. Dong, Chem. Commun. 49 (2013) 2503–2505.
[14] H. Bao, Y. Pan, Y. Ping, N.G. Sahoo, T. Wu, L. Li, J. Li, L.H. Gan, Small 7 (2011) 1569–1578.
[15] W. Miao, G. Shim, C.M. Kang, S. Lee, Y.S. Choe, H. Choi, Y. Oh, Biomaterials 34 (2013) 9638–9647.
[16] L. Zhang, Z. Wang, Z. Lu, H. Shen, J. Huang, Q. Zhao, M. Liu, N. He, Z. Zhang, J. Mater. Chem. B 1 (2013) 749–755.
[17] M. Pumera, A. Ambrosi, A. Bonanni, E.L.K. Chng, H.L. Poh, TrAC, Trends Anal. Chem. 29 (2010) 954–965.
[18] G. Yang, J. Cao, L. Li, R.K. Rana, J. Zhu, Carbon 51 (2013) 124–133.
[19] J. Wang, Y. Zhao, F. Ma, K. Wang, F. Wang, X. Xia, J. Mater. Chem. B 1 (2013) 1406–1413.
[20] D.R. Dreyer, S.J. Park, C.W. Bielawski, R.S. Ruoff, Chem. Soc. Rev. 39 (2010) 228–240.
[21] Y. Zhu, S. Murali, W. Cai, X. Li, J.W. Suk, J.R. Potts, R.S. Ruoff, Adv. Mater. 22 (2010) 3906–3924.
[22] Y. Yan, Z. Zheng, C. Deng, Y. Li, X. Zhang, P. Yang, Anal. Chem. 85 (2013) 8483–8487.
[23] Y. Liu, J. Liu, P. Yin, M. Gao, C. Deng, X. Zhang, J. Mass Spectrom. 46 (2011) 804–815.
[24] H. Bo, Q. Chen, L. Zhang, G. Chen, Analyst 136 (2012) 5190–5196.
[25] B. Jiang, K. Yang, Q. Zhao, Q. Wu, Z. Liang, L. Zhang, X. Peng, Y. Zhang, J. Chromatogr. A 1254 (2012) 8–13.
[26] G. Xu, X. Chen, J. Hu, P. Yang, D. Yang, L. Wei, Analyst 137 (2012) 2757–2761.
[27] H. Bo, L. Zhang, G. Chen, J. Chromatogr. A 1310 (2013) 74–78.
[28] W. Lesniak, A.U. Bielinska, K. Sun, K.W. Janczak, X. Shi, J.R. Baker, L.P. Balogh, Nano Lett. 5 (2005) 2123–2130.
[29] S. Wen, K. Li, H. Cai, Q. Chen, M. Shen, Y. Huang, C. Peng, W. Hou, M. Zhu, G. Zhang, X. Shi, Biomaterials 34 (2013) 1570–1580.
[30] X. Shi, S. Wang, H. Sun, J.R.B. , Soft Matter 3 (2007) 71–74.
[31] M.E. Garcia, L.A. Baker, R.M. Crooks, Anal. Chem. 71 (1999) 256–258.
[32] P.S. Wate, S.S. Banerjee, A. Jalota-Badhwar, R.R. Mascarenhas, K.R. Zope, J. Khandare, R.D.K. Misra, Nanotechnology 23 (2012) 415101.
[33] J.M. Kim, J. Kim., J. Kim, Chem. Commun. 48 (2012) 9233–9235.
[34] K. Jayakumar, R. Rajesh, V. Dharuman, R. Venkatasan, J.H. Hahn, S.K. Pandian, Biosens. Bioelectron. 31 (2012) 406–412.
[35] S. Yang, X. Feng, S. Ivanovici, K. Müllen, Angew. Chem. Int. Ed. 49 (2010) 8408–8411.
[36] X. Yang, X. Zhang, Y. Ma, Y. Huang, Y. Wang, Y. Chen, J. Mater. Chem. 19 (2009) 2710–2714.
[37] B. Li, H. Cao, J. Shao, M. Qu, J.H. Warner, J. Mater. Chem. 21 (2011) 5069–5075.
[38] H Yang, Q Zhang, C. Shan, F. Li, D. Han, L. Niu, Langmuir 26 (2010) 6708–6712.
[39] D.C. Marcano, D.V. Kosynkin, J.M. Berlin, A. Sinitskii, Z. Sun, A. Slesarev, L. B. Alemany, W. Lu, J.M. Tour, ACS Nano 8 (2010) 4806–4814.
[40] F. He, J. Fan, D. Ma, L Zhang, C. Leung, H.L. Chan, Carbon 48 (2010) 3139–3144.
[41] S. Lin, D. Yun, D. Qi, C. Deng, Y. Li, X. Zhang, J. Proteome Res. 7 (2008) 1297–1307.